

Catalytic, biological and DNA binding studies of organotin(IV) carboxylates of 3-(2-fluorophenyl)-2-methylacrylic acid: Synthesis, spectroscopic characterization and X-ray structure analysis

Muhammad Tariq^{a,*}, Saqib Ali^{a,*}, Naseer Ali Shah^b, Niaz Muhammad^c, Muhammad Nawaz Tahir^d, Nasir Khalid^e, Muhammad Rashid Khan^b

^a Department of Chemistry, Quaid-i-Azam University, Islamabad 45320, Pakistan

^b Department of Biochemistry, Quaid-i-Azam University, Islamabad 45320, Pakistan

^c Department of Chemistry, Abdul Wali Khan University, Mardan, Pakistan

^d Department of Physics, University of Sargodha, Sargodha, Pakistan

^e Chemistry Division, Pakistan Institute of Nuclear Science and Technology, P.O. Nilore, Islamabad, Pakistan

ARTICLE INFO

Article history:

Received 3 March 2013

Accepted 11 April 2013

Available online 19 April 2013

Keywords:

Organotin(IV) carboxylate
Antibacterial activity
Antifungal activity
Transesterification
Crystal structure

ABSTRACT

A new series of organotin(IV) carboxylates [Me₂SnL₂] (**1**), [Bu₂SnL₂] (**2**), [Oct₂SnL₂] (**3**), [Me₃SnL] (**4**), [Bu₃SnL] (**5**) and [Ph₃SnL] (**6**), where L = 3-(2-fluorophenyl)-2-methylacrylate have been synthesized and characterized by FT-IR, CHNS and NMR (¹H, ¹³C). The crystal structures of complexes (**1**) and (**4**) were also analyzed by single crystal X-ray analysis. The complex (**1**) adopted distorted octahedral geometry while complex (**4**) exhibited distorted trigonal bipyramidal geometry. The catalytic activity of the complexes was assessed in the production of biodiesel. Biodiesel is the monoalkyl ester of long chain fatty acids derived from the renewable feed stock, such as vegetable oil and is produced by a transesterification of vegetable oil with methanol. The results revealed that triorganotin(IV) complexes showed better catalytic activity than their diorganotin(IV) analogues. The complexes were also screened for their biological activities such as antibacterial, antifungal and cytotoxicity. The complexes **4–6** showed significant activity than the complexes **1–3**. DNA interactions studies of ligand and complexes were investigated by UV–Vis absorption spectroscopy. The results showed that both ligand and complexes interact with DNA via intercalation as well as minor groove binding.

© 2013 Elsevier Ltd. All rights reserved.

1. Introduction

The organotin compounds have been used as pesticides, fungicides, bactericides, homogeneous catalysts and in the synthesis of polyesters, polyurethanes etc. [1–7]. The broad spectrum biological and non-biological applications depend on both nature of molecule and coordination number of tin atom [8–11]. Otera used organostannyl and organodistannoxnae isothiocyanates as catalysts in transesterification of ester with alcohol [12]. However, less attention has been devoted on catalytic activity of organotin(IV) carboxylates in transesterification of triglycerides (vegetable oil) into fatty acid methyl esters (biodiesel). Biodiesel is the monoalkyl ester of long chain fatty acids derived from the renewable feed stock, such as vegetable oil or animal fats and is usually produced by a transesterification of triglycerides (vegetable oil) with methanol [13–15].

In view of the biocidal and catalytic activities of organotin(IV) carboxylates, we have synthesized a series of di and

triorganotin(IV) carboxylates of the type R_{4–n}SnL_n where R = Me, n-Bu, Ph, L = 3-(2-fluorophenyl)-2-methylacrylate and n = 1 or 2. These complexes were characterized by FT-IR, CHNS, NMR (¹H, ¹³C) and single X-ray crystal analysis. The catalytic activity of the complexes was assessed in transesterification of triglycerides (vegetable oil) into fatty acid methyl esters (biodiesel). The complexes were screened for their anti-bacterial, anti-fungal and cytotoxicity. DNA interaction studies were also performed using UV–Vis spectrophotometer to find out drug–DNA mechanism.

2. Experimental

2.1. Materials and methods

All the di- and triorganotin(IV) precursors were purchased from Sigma–Aldrich and were used without further purification. All the solvents purchased from Merck (Germany) were of analytical grade and dried according to reported procedures before use [16]. The melting points were measured on a Gallenkamp (UK) electrothermal melting point apparatus. Microanalyses were done using a

* Corresponding authors. Tel.: +92 51 90642130; fax: +92 51 90642241.

E-mail addresses: mtnazir@yahoo.com (M. Tariq), drsa54@yahoo.com (S. Ali).

Leo CHNS 932 apparatus. IR spectra were recorded in the range from 4000 to 400 cm^{-1} using a Thermo Nicolet-6700 FT-IR Spectrophotometer using KBr discs. ^1H and ^{13}C NMR spectra were recorded at room temperature in CDCl_3 on a Bruker Avance Digital 300 MHz NMR spectrometer (Switzerland). The X-ray diffraction data were collected on a Bruker SMART APEX CCD diffractometer, equipped with a 4 K CCD detector set 60.0 mm from the crystal. The crystals were cooled to 100 ± 1 K using the Bruker KRYOFLEX low temperature device and intensity measurements were performed using graphite monochromated Mo $K\alpha$ radiation from a sealed ceramic diffraction tube (SIEMENS). Generator settings were 50 kV/40 mA. The structure was solved by Patterson method and extension of the model was accomplished by direct method using the program DIRDIF or SIR2004. Final refinement on F^2 was carried out by full matrix least square techniques using SHELXL-97, a modified version of the program PLUTO (preparation of illustrations) and PLATON package. The absorption spectra were recorded on a Shimadzu 1800 UV-Vis spectrophotometer. The sesame seeds were purchased from a local market. The seeds were washed with distilled water to remove the dirt and were oven dried at 60 °C till constant weight. The oil was extracted by using German made electric oil expeller (KEK P0015-10127).

2.2. Syntheses

2.2.1. Synthesis of 3-(2-fluorophenyl) 2-methylacrylic acid

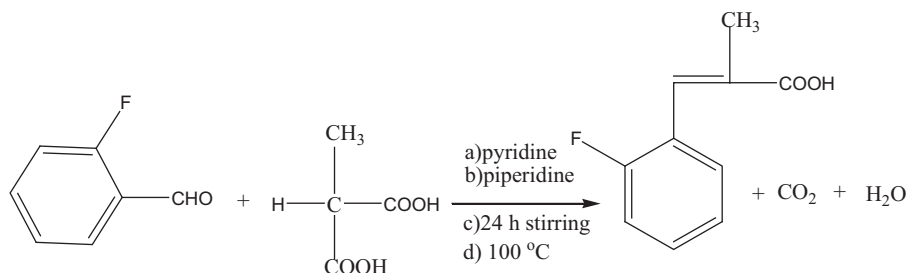
The mixture of 2-fluorobenzaldehyde (3.47 g, 28 mmol), methylmalonic acid (6.61 g, 56 mmol) and piperidine (4.76 g, 56 mmol) in molar ratios of 1:2:2 (scheme 1) was refluxed in two neck round bottom flask in pyridine as solvent for 24 h on steam bath. After cooling, the reaction mixture was poured into ice water and added conc. HCl until pH 3. The precipitates formed were filtered, washed with water, recrystallized in ethanol and dried.

Yield: 3.49 g, 69.3%. M.p. 75–77 °C. *Anal. Calc.* for $\text{C}_{10}\text{H}_9\text{O}_2\text{F}$: C, 66.66; H, 5.03. *Found:* C, 66.23; H, 5.0%. IR (KBr, cm^{-1}): 3321 $\nu(\text{OH})$, 1672 $\nu(\text{OCO})_{\text{asym}}$, 1421 $\nu(\text{OCO})_{\text{sym}}$, ($\Delta\nu = 251 \text{ cm}^{-1}$). ^1H NMR (CDCl_3 , ppm): 11.00 (s, H_1 , 1H), 7.90 (s, H_3 , 1H), 7.10–7.45 Ar-H (m, H_{6-9} , 4H), 2.10 (s, H_{10} , 3H). ^{13}C NMR (CDCl_3 , ppm): 173.8 (C-1), 123.4 (C-2), 140.5 (C-3), 129.9 (C-4), 162.0, 158.7 (C-5), 115.6 (C-6), 133.9 (C-7), 130.4 (C-8), 130.6 (C-9) 13.9 (C-10).

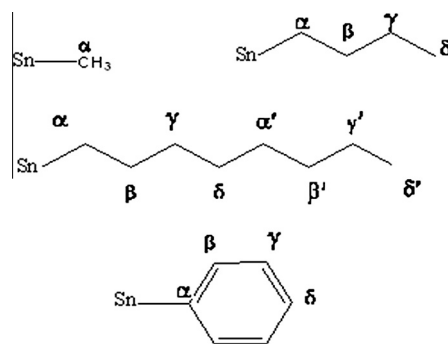
2.2.2. Synthesis of Na-salt of 3-(2-fluorophenyl)-2-methylacrylic acid

The sodium salt of ligand, $\text{R}'\text{COONa}$, was prepared by dropwise addition of an equimolar amount of sodium hydrogen carbonate solution to a methanolic solution of ligand acid ($\text{R}'\text{COOH}$). The solution was stirred for 2 h at room temperature, evaporated under reduced pressure to give a white solid and was vacuum dried.

Scheme 2 represents numbering in ligand and R groups attached to Sn atom for ^1H and ^{13}C NMR interpretation



Scheme 1.

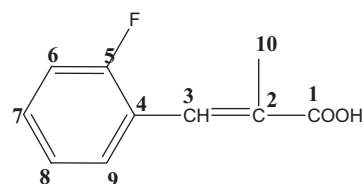


2.2.3. Dimethyltin(IV) bis[3-(2-fluorophenyl)-2-methylacrylate] (1)

The sodium salt $\text{R}'\text{COONa}$ (0.404 g, 2.0 mmol), was refluxed with dimethyltin(IV) dichloride (0.219 g, 1.0 mmol) in dry toluene contained in a 250 mL two necked round bottom flask for 10 h. A turbid solution obtained, was left overnight at room temperature. The sodium chloride formed was filtered off and the filtrate was rotary evaporated. The resultant solid mass was recrystallized from chloroform and *n*-hexane (4:1) mixture. Yield: 0.41 g, 82%. M.p. 117–118 °C. *Anal. Calc.* for $\text{C}_{22}\text{H}_{22}\text{F}_2\text{O}_4\text{Sn}$: C, 52.11; H, 4.37. *Found:* C, 52.01; H, 4.28%. IR (KBr, cm^{-1}): 1573 $\nu(\text{OCO})_{\text{asym}}$, 1452 $\nu(\text{OCO})_{\text{sym}}$, ($\Delta\nu = 121 \text{ cm}^{-1}$), 524.0 $\nu(\text{Sn}-\text{C})$, 448.0 $\nu(\text{Sn}-\text{O})$. ^1H NMR (CDCl_3 , ppm): 7.89 (s, H_3 , 2H), 7.09–7.42 (m, Ar- H_{6-9} , 8H), 2.10 (s, H_{10} , 6H), 1.12 (s, $\text{H}\alpha$, 6H), $^2J(^{119}/^{117}\text{Sn}-^1\text{H}) = 83/80 \text{ Hz}$. ^{13}C NMR (CDCl_3 , ppm): 177.2 (C-1), 123.6 (C-2), 140.7 (C-3), 130.5 (C-4), 162.0, 158.7 (C-5), 115.5 (C-6), 133.5 (C-7), 123.8 (C-8), 130.2 (C-9), 14.5 (C-10), 4.6 (C- α), $^1J(^{119}/^{117}\text{Sn}-^{13}\text{C}) = 760 \text{ Hz}$.

2.2.4. Dibutyltin(IV) bis[3-(2-fluorophenyl) 2-methylacrylate] (2)

Compound 2 was prepared in the same way as 1, using $\text{R}'\text{COONa}$ (0.404 g, 2.0 mmol) and dibutyltin(IV) dichloride (0.303 g, 1.0 mmol). The product was recrystallized from chloroform and *n*-hexane (4:1) mixture. Yield: 0.45 g, 76%. M.p. 102–104 °C. *Anal. Calc.* for $\text{C}_{28}\text{H}_{34}\text{F}_2\text{O}_4\text{Sn}$: C, 56.88; H, 5.80. *Found:* C, 56.18; H, 5.65%. IR (KBr, cm^{-1}): 1574 $\nu(\text{OCO})_{\text{asym}}$, 1452 $\nu(\text{OCO})_{\text{sym}}$, ($\Delta\nu = 122 \text{ cm}^{-1}$), 525 $\nu(\text{Sn}-\text{C})$, 447 $\nu(\text{Sn}-\text{O})$. ^1H NMR (CDCl_3 , ppm): 7.88 (s, H_3 , 2H), 7.06–7.42 (m, Ar- H_{6-9} , 8H), 2.10 (s, H_{10} , 6H), 1.78 (t, $\text{H}\alpha$, 4H), 1.48–1.41 (m, $\text{H}_{\beta-\gamma}$, 8H), 0.92 (t, H_δ , 6H). ^{13}C NMR (CDCl_3 , ppm): 177.6 (C-1), 123.8 (C-2), 141.0 (C-3), 126.8



Scheme 2.

(C-4), 162.0, 158.7 (C-5), 115.8 (C-6), 133.0 (C-7), 123.9 (C-8), 129.7 (C-9), 14.6 (C-10), 21.4 (C- α), 25.4 (C- β), 29.1 (C- γ), 13.5 (C- δ).

2.2.5. Diocetyl tin(IV) bis[(3-(2-fluorophenyl) 2-methylacrylate)] (3)

Compound **3** was prepared by using ligand acid, R'COOH (0.36 g, 2.0 mmol) and diocetyl tin(IV) oxide (0.36 g, 1.0 mmol). The reactant mixture was suspended in 100 mL dry toluene in a single necked round bottom flask (250 mL), equipped with a Dean–Stark apparatus. The mixture was refluxed for 10 h and water formed during the condensation reaction was removed at regular intervals. A clear solution thus obtained, was cooled to room temperature and solvent was removed under reduced pressure. The solid obtained was recrystallized from chloroform and *n*-hexane (4:1) mixture. Yield: 0.48 g, 68%. M.p. gel. *Anal.* Calc. for C₃₆H₅₀F₂O₄Sn: C, 61.46; H, 7.16. Found: C, 60.25; H, 7.02%. IR (KBr, cm⁻¹): 1574 ν (OCO)_{asym}, 1453 ν (OCO)_{sym}, ($\Delta\nu = 121$ cm⁻¹), 522.5 ν (Sn–C), 441 ν (Sn–O). ¹H NMR (CDCl₃, ppm): 7.88 (s, H₃, 2H), 7.08–7.43 (m, Ar–H_{6–9}, 8H), 2.11 (s, H₁₀, 6H), 1.78–1.27 (bs, H _{$\alpha,\beta,\gamma,\delta,\alpha',\beta',\gamma'$} , 28H), 0.85 (t, H _{$\delta'$} , 6H). ¹³C NMR (CDCl₃, ppm): 177.6 (C-1), 123.7 (C-2), 140.8 (C-3), 130.0 (C-4), 162.0, 158.7 (C-5), 115.5 (C-6), 133.0 (C-7), 124.0 (C-8), 130.6 (C-9), 14.7 (C-10), 25.6 (C- α), 24.4 (C- β), 33.9 (C- γ), 31.8 (C- δ), 29.7 (C- α'), 29.0 (C- β'), 22.5 (C- γ'), 14.0 (C- δ').

2.2.6. Trimethyl tin(IV) 3-(2-fluorophenyl) 2-methylacrylate (4)

Compound **4** was prepared in the same way as **1**, using R'COONa (0.404 g, 2.0 mmol) and trimethyl tin(IV) chloride (0.398 g, 2.0 mmol). The product was recrystallized from chloroform and *n*-hexane (4:1) mixture. Yield: 0.56 g, 81%. M.p. 125–126 °C. *Anal.* Calc. for C₁₃H₁₇FO₂Sn: C, 45.52; H, 5.0. Found: C, 45.13; H, 4.90%. IR (KBr, cm⁻¹): 1574 ν (OCO)_{asym}, 1387 ν (OCO)_{sym}, ($\Delta\nu = 187$ cm⁻¹), 524.0 ν (Sn–C), 444 ν (Sn–O). ¹H NMR (CDCl₃, ppm): 7.72 (s, H₃, 1H), 7.06–7.40 (m, Ar–H_{6–9}, 4H), 2.05 (s, H₁₀, 3H), 0.62 (s, H _{α} , 9H) ²J(¹¹⁹/¹¹⁷Sn–¹H) = [58/56 Hz]. ¹³C NMR (CDCl₃, ppm): 173.3 (C-1), 123.6 (C-2), 141.2 (C-3), 129.6 (C-4), 161.9, 158.6 (C-5), 115.4 (C-6), 132.3 (C-7), 124.4 (C-8), 130.9 (C-9), 14.8 (C-10), –2.3 (C- α), ¹J(¹¹⁹Sn–C) = [396/378 Hz].

2.2.7. Tributyl tin(IV) 3-(2-fluorophenyl)-2-methylacrylate (5)

Compound **5** was prepared in the same way as **1**, using R'COONa (0.404 g, 2.0 mmol) and tributyl tin(IV) chloride (0.650 g, 2.0 mmol). The product was recrystallized from chloroform and *n*-hexane (4:1) mixture. Yield: 0.72 g, 76%. M.p. 139–141 °C. *Anal.* Calc. for C₂₂H₃₅FO₂Sn: C, 56.31; H, 7.52. Found: C, 55.98; H, 7.14%. IR (KBr, cm⁻¹): 1560 ν (OCO)_{asym}, 1373 ν (OCO)_{sym}, ($\Delta\nu = 187$ cm⁻¹), 522.2 ν (Sn–C), 441 ν (Sn–O). ¹H NMR (CDCl₃, ppm): 7.88 (s, H₃, 1H), 7.08–7.42 (m, Ar–H_{6–9}, 4H), 2.09 (s, H₁₀, 3H), 1.82–1.79 (t, H _{α} , 6H), 1.47–1.40 (m, H _{β} , γ , 12H), 0.94 (t, H _{δ} , 9H). ¹³C NMR (CDCl₃): 177.6 (C-1), 123.4 (C-2), 140.3 (C-3), 129.3 (C-4), 162.0, 158.7 (C-5), 115.6 (C-6), 130.5 (C-7), 123.8 (C-8), 130.4 (C-9), 14.5 (C-10), 25.7 (C- α), 29.5 (C- β), 32.8 (C- γ), 14.2 (C- δ).

2.2.8. Triphenyl tin(IV) 3-(2-fluorophenyl)-2-methylacrylate (6)

Compound **6** was prepared in the same way as **1**, using R'COONa (0.404 g, 2.0 mmol) and triphenyl tin(IV) chloride (0.77 g, 2.0 mmol). The product was recrystallized from chloroform and *n*-hexane (4:1) mixture. Yield: 0.82 g, 78%. M.p. 146–148 °C. *Anal.* Calc. for C₂₈H₂₃FO₂Sn: C, 63.55; H, 4.38. Found: C, 63.18; H, 4.08%. IR (KBr, cm⁻¹): 1643 ν (OCO)_{asym}, 1482 ν (OCO)_{sym}, ($\Delta\nu = 161$ cm⁻¹), 443 ν (Sn–O). ¹H NMR (CDCl₃, ppm): 7.68 (s, H₃, 1H), 7.16–7.47 (m, Ar–H_{6–9}, 4H), 2.17 (s, H₁₀, 3H), 7.80–7.71 (H _{β} , H γ , H δ , 15H). ¹³C NMR (CDCl₃, ppm): 175.7 (C-1), 123.2 (C-2), 140.1 (C-3), 130.4 (C-4), 161.5, 158.6 (C-5), 115.3 (C-6), 133.6 (C-7), 124.1 (C-8), 130.5 (C-9), 14.1 (C-10), 139.7 (C- α), 137.2 (C- β), 129.7 (C- γ), 130.3 (C- δ).

2.3. Antibacterial studies

The antibacterial activity of ligand HL and its organotin(IV) complexes were tested against four bacterial strains; two Gram-Positive (*Micrococcus luteus* and *Staphylococcus aureus*) and three Gram-negative (*Escherichia coli* and *Bordetella bronchiseptica*). The agar well-diffusion method was used in which Broth culture (0.75 mL) containing ca. 10⁶ colony forming units (CFU) per mL of the test strain was added to 75 mL of nutrient agar medium at 45 °C, mixed well, and then poured into a 14 cm sterile petri plate [17]. The media was allowed to solidify, and 8 mm wells were dug with a sterile metallic borer. Then a DMSO solution of test sample (100 μ L) at 1 mg/mL was added to the respective wells. DMSO served as negative control, and the standard antibacterial drugs *Roxythromycin* (1 mg/mL) and *Cefixime* (1 mg/mL) were used as positive control. Triplicate plates of each bacterial strain were prepared which were incubated aerobically at 37 °C for 24 h. The activity was determined by measuring the diameter of zone showing complete inhibition (mm).

2.4. Antifungal studies

Antifungal activity against four fungal strains (*Aspergillus Flavus*, *Aspergillus niger*, *Fusarium solani* and *Aspergillus fumigatus*) was determined by using agar tube dilution method [18]. Screw capped test tubes containing Sabouraud dextrose agar (SDA) medium (4 mL) were autoclaved at 121 °C for 15 min. Tubes were allowed to cool at 50 °C and non solidified SDA was loaded with 66.6 μ L of compound from the stock solution (12 mg/mL in DMSO) to make 200 μ g/mL final concentration. Tubes were then allowed to solidify in slanting position at room temperature. Each tube was inoculated with 4 mm diameter piece of inoculum from seven days old fungal culture. The media supplemented with DMSO and *Turbinafine* (200 μ g/mL) were used as negative and positive control, respectively. The tubes were incubated at 28 °C for 7 days and growth was determined by measuring linear growth (mm) and growth inhibition was calculated with reference to growth in vehicle control as shown in equation.

$$\% \text{ Growth inhibition} = 100 - \left(\frac{\text{Linear growth in test sample (mm)}}{\text{Linear growth in control (mm)}} \times 100 \right)$$

2.5. Cytotoxic studies

Cytotoxicity was studied by the brine-shrimp lethality assay method [17]. Brine-shrimp (*Artemia salina*) eggs were hatched in artificial sea water (3.8 g sea salt/L) at ambient temperature of 23 \pm 1 °C. After 2 days these shrimps were transferred to vials containing 5 mL of artificial sea water (10 shrimps per vial) with 10, 100 and 500 μ g/mL final concentrations of each compound taken from their stock solutions of 12 mg/mL in DMSO. After 24 h number of surviving shrimps was counted. Data was analyzed with a Biostat 2009 computer programme (Probit analysis) to determine LD₅₀ values.

2.6. Catalytic experiment

Transesterification of sesame oil was carried out using organotin(IV) carboxylate as catalysts in molar ratio of 400:100:1 (methanol:oil:catalyst) [5]. 0.01 mol sesame oil was transesterified using 0.04 mol methanol and 0.1 mmol catalyst in a 100 mL three neck round bottom flask equipped with reflux condenser, magnetic stirrer, thermometer and sampling outlet. Before the reaction, the organotin catalyst was solubilized in 0.5 mL chloroform. The reaction mixture was refluxed with constant stirring. The sample was taken after 1, 8, 16 and 24 h and was analyzed by ¹H NMR to check

the % age conversion of triglycerides in sesame oil into fatty acid methyl esters (biodiesel).

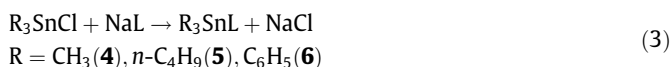
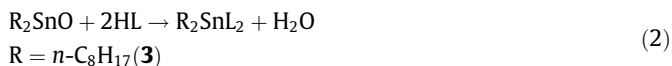
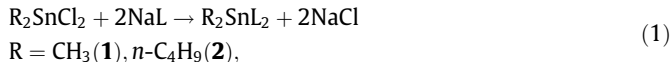
2.7. DNA interaction studies by UV–Vis spectroscopy

0.2 g of SS-DNA (salmon sperm) was dissolved in 100 mL of double deionized water and kept at 4 °C. Solutions of DNA in 20 mM Tris–HCl (pH 7.4) gave the ratio of UV absorbance at 260 and 280 nm, A_{260}/A_{280} , of 1.86 indicating that the DNA is sufficiently free from protein [19]. The DNA concentration was determined via absorption spectroscopy using the molar absorption coefficient of $6600 \text{ M}^{-1} \text{ cm}^{-1}$ at 260 nm [20], and was found as $7.45 \times 10^{-5} \text{ M}$. From this stock solution 3, 6, 9, 12, 15, 18, 21, 24 and 27 μM working solutions were prepared by dilution method. The ligand **HL**, complexes **1** and **4** were dissolved in 10% DMSO at a concentration of $5 \times 10^{-5} \text{ M}$. The UV absorption titrations were performed by keeping the complex concentration fixed while varying the concentration of DNA. Equivalent solutions of DNA were added to the complex and reference solutions to eliminate the absorbance of DNA itself. Compound-DNA solutions were allowed to incubate for 30 min at ambient temperature before measurements were made. Absorption spectra were recorded using cuvettes of 1 cm path length.

3. Results and discussions

3.1. Syntheses of complexes 1–6

Diorganotin dichloride and triorganotin chloride with NaL in 1:2 and 1:1 M ratios, respectively while R_2SnO with **HL** in 1:2 M ratios give complexes according to the following equations



3.2. FT-IR analysis

The binding mode of ligand to tin atom was determined using FT-IR spectra in the range $4000\text{--}400 \text{ cm}^{-1}$ by the difference between the asymmetric and symmetric carboxylate stretching vibrations [$\Delta\nu = \nu_{\text{asym}}(\text{COO}^-) - \nu_{\text{sym}}(\text{COO}^-)$] [21]. It is generally believed that the difference in $\Delta\nu$ between asymmetric (COO^-) and symmetric (COO^-) absorption frequencies below 200 cm^{-1} indicates the bidentate carboxylate moiety, but greater than 200 cm^{-1} indicates the unidentate carboxylate moiety [22]. The magnitudes of $\Delta\nu$ [$(\nu_{\text{asym}}(\text{COO}^-) - \nu_{\text{sym}}(\text{COO}^-))$] for complexes **1–6** are within range of $121\text{--}187 \text{ cm}^{-1}$ which indicate the presence of bidentate carboxylate groups in these complexes [23]. The absorption bands in the $441\text{--}470 \text{ cm}^{-1}$ region are assigned to the stretching mode of the Sn–O linkage which indicates the formation of complexes [24].

3.3. NMR studies

3.3.1. ^1H NMR studies

The chemical shift, multiplicities pattern in ^1H NMR spectra are helpful in elucidation of structures of the synthesized compounds. All the protons present in the synthesized ligand and compounds (**1–6**) were identified by the position and number

with the protons calculated from incremental method. The satellites due to ($^{119/117}\text{Sn}$, ^1H) coupling are helpful in finding geometry around tin in solution. The methyl protons of dimethyltin(IV) (**1**) and trimethyltin(IV) (**4**) derivative appear as sharp singlets with well defined satellites in the range 0.99–1.26 and 0.53–0.72 ppm having coupling constants of 83/80 and 58/56 Hz [2J ($^{119/117}\text{Sn}$, ^1H)], respectively. The determined 2J values indicate five or six coordination for compound (**1**) and four co-ordination for compound (**4**) around tin atom in solution state. The protons of n -butyltin(IV) derivative mostly show a complex pattern and were assigned according to the literature [25,26]. Despite the complex pattern of ^1H NMR spectra of di- (**2**) and tri- n -butyltin(IV) (**5**) derivatives, a clear triplet due to terminal methyl group appears in the range of 0.92–0.94 ppm. The methylene protons (CH_2) of n -octyltin(IV) derivative (**3**) exhibit somewhat different behavior compared with the n -butyl groups of the respective complexes. All the CH_2 protons of n -octyl groups give broad/multiplet signals in the range 0.85–1.78 ppm.

3.3.2. ^{13}C NMR studies

In ^{13}C NMR, the carbon signals of synthesized ligand and its organotin(IV) derivatives are in good agreement with expected values. The carbon attached to fluoro group and others in its vicinity gave doublets due to heteronuclear coupling of [^{13}C , ^{19}F]. The carbons bonded to Sn atom have satellites due to 1J [^{119}Sn , ^{13}C] couplings which are important parameters for characterization of organotin(IV) compounds and geometry around tin atom. For dimethyl derivative (**1**), the value of 1J [^{119}Sn , ^{13}C] is 760 Hz while for trimethyltin(IV) (**4**), it is 388 Hz which confirm six co-ordination geometry around the tin in solution for (**1**) and four coordination for (**4**), respectively, [27,28].

3.4. Crystal structures of complexes 1 and 4

The dimeric structure and packing diagram of complex **1** are shown in Figs. 1 and 2 while the crystal data, selected bond lengths and bond angles of complex **1** are listed in Tables 1 and 2, respectively. The four oxygen atoms from two carboxylate ligands are in planar position. The carboxylate moiety COO^- of ligand is bonded in anisobidentate mode with two shorter bonds (Sn1–O1, Sn1–O3) and two longer bonds (Sn1–O2 and Sn1–O4) in asymmetric way as depicted in Table 2. The longer Sn–O distances (Sn1–O2 = 2.6543 Å and Sn1–O4 = 2.575 Å) are significantly less than the sum of the van der Waal's radii (3.68 Å) [29]. The asymmetric mode of coordination of the carboxylate ligands is further confirmed by unequal C–O bond distances; O1–C1 = 1.298(3) Å, O2–C1 = 1.224(3) Å and

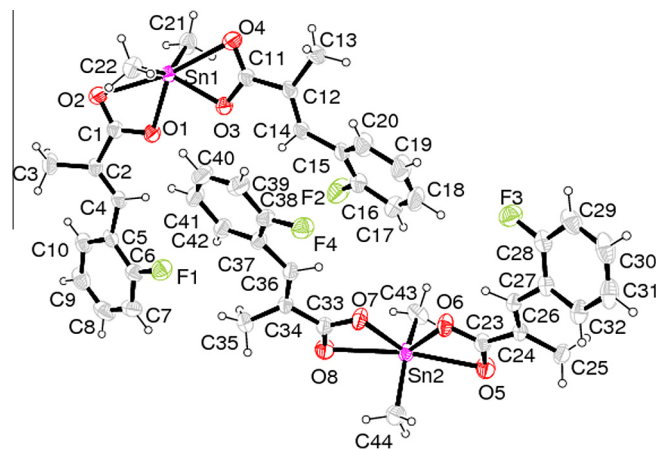


Fig. 1. Dimeric ORTEP diagram of complex 1.

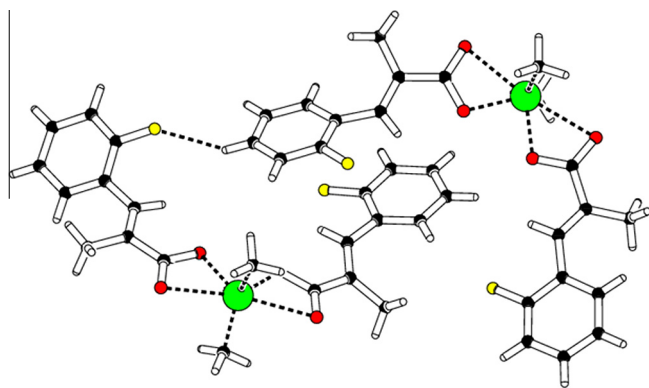


Fig. 2. Platon dimeric diagram of complex 1.

O3–C11 = 1.295(3) Å, O4–C11 = 1.232(3) Å as shown in Table 2. The two methyl groups attached to tin atom occupy axial position with C21–Sn–C22 angle 143.95(12)° which shows that methyl groups do not occupy the exact axial positions. The two methyl groups in distorted axial position and four oxygen atoms from the two chelating carboxylate ligands in basal plane represent skew-trapezoidal or distorted octahedral geometry around tin [5,30]. The geometry, bond lengths and angles are comparable with literature values [5,31–33].

The dimeric structure and polymeric bridging diagram of complex 4 are shown in Figs. 3 and 4, while the crystal data, selected bond length and bond angles are listed in Tables 1 and 3, respectively. The complex 4 showed polymeric structure with distorted trigonal bipyramidal geometry. The three methyl groups attached to tin atom are in trigonal plane having C–Sn–C angle 113.2° to 126.6° while two oxygen atoms of bridging carboxylate ligands occupy axial position with O–Sn–O angle 175.06°. Thus carboxylate ligand bridges the two symmetry related Sn atoms and gives rise to the unequal Sn–O bond distances which is further reflected from C–O bond lengths, the shorter C–O bond is involved in the longer Sn–O interaction and *vice versa*. These bond lengths and polymeric bridging behavior are comparable with literature

[5,34,35]. The 2-fluorophenyl ring (C18a–C23a/F2a and C18b–C23b/F2b) is disordered over two sites with refined occupancy ratio of 0.711(7):0.289(7). The disordered benzene rings were idealized as regular hexagon of bond length 1.39 Å and these C-atoms were treated having equal anisotropic thermal parameters. In a similar manner the disordered F-atoms were treated having equal anisotropic thermal parameters. The geometry around Sn can be deduced by the value of $\tau = (\beta - \alpha)/60$, where β is the largest and α is the second largest basal angles around the Sn atom [36]. The angle values $\alpha = \beta = 180^\circ$ correspond to τ value equal to zero for a perfect square-pyramidal and the value of $\alpha = 120^\circ$ and $\beta = 180^\circ$ correspond to τ value equal to 1 for a perfect trigonal-bipyramidal geometry. The calculated τ value for complex 4 is 0.81 which indicates distorted trigonal-bipyramidal geometry around the Sn atom.

3.5. Biological studies

3.5.1. Antibacterial studies

In vitro antibacterial activity tests of the ligand HL and its organotin(IV) complexes (1–6) were carried out against four bacterial strains; two Gram-Positive (*Micrococcus luteus* and *Staphylococcus*

Table 2
Selected bond lengths (Å) and bond angles (°) of complex 1.

Bond lengths (Å)			
Sn1–C21	2.086(3)	O3–C11	1.295(3)
Sn1–C22	2.092(3)	O4–C11	1.232(4)
Sn1–O1	2.0757(19)	Sn2–O5	2.566(2)
Sn1–O2	2.6543(18)	Sn2–O6	2.0781(17)
Sn1–O3	2.0857(17)	Sn2–O7	2.0780(19)
Sn1–O4	2.575(2)	Sn2–O8	2.6698(19)
O2–C1	1.224(3)	Sn2–C44	2.088(3)
O1–C1	1.298(3)		
Bond angles (°)			
O1–Sn1–O2	53.18(6)	O1–Sn1–C21	104.90(10)
O1–Sn1–O3	81.99(7)	O1–Sn1–C22	101.72(10)
O2–Sn1–O3	135.16(7)	O2–Sn1–C21	90.84(9)
O2–Sn1–O4	169.74(6)	O2–Sn1–C22	85.97(9)
O1–Sn1–O4	136.36(7)	O3–Sn1–C21	101.27(10)
C21–Sn1–C22	143.95(12)	O3–Sn1–C22	106.18(9)

Table 1
Crystal data and structure refinement parameters for complexes 1 and 4.

Compound	1	4
Chemical formula	C ₂₂ H ₂₂ F ₂ O ₄ Sn	C ₁₃ H ₁₇ FO ₂ Sn
Formula mass (g mol ⁻¹)	507.11	342.96
Crystal system	monoclinic	triclinic
Space group	P2 ₁ /c	P1
Unit cell dimensions		
a (Å)	13.5161(3)	9.8854(3)
b (Å)	23.0786(6)	11.5996(5)
c (Å)	13.9395(3)	13.9493(6)
α (°)	90.00	99.922(2)
β (°)	96.976(1)	109.989(1)
γ (°)	90.00	101.495(2)
V (Å ³)	4316.00(17)	1421.92(10)
Z	8	2
T (K)	296(2)	296(2)
D _{calc} (g cm ⁻³)	1.561	1.602
Absorption coefficient (mm ⁻¹)	1.225	1.797
F(000)	2032	680
Radiation (Å ⁰) (Mo K α)	0.71073	0.71073
Index ranges	-16 ≤ h ≤ 16, -28 ≤ k ≤ 28, -17 ≤ l ≤ 17	-12 ≤ h ≤ 12, -14 ≤ k ≤ 14, -17 ≤ l ≤ 17
θ (°) Min max	1.52–26.0	1.86–26.0
Total reflections	8485	5570
Restraints/parameters	0/531	0/316
R _{all} , R _{gt}	0.0396, 0.0261	0.0466, 0.0351
wR _{ref} , wR _{gt}	0.0649, 0.0583	0.0945, 0.0865
Goodness-of-fit (GOF) on F ²	1.004	1.053

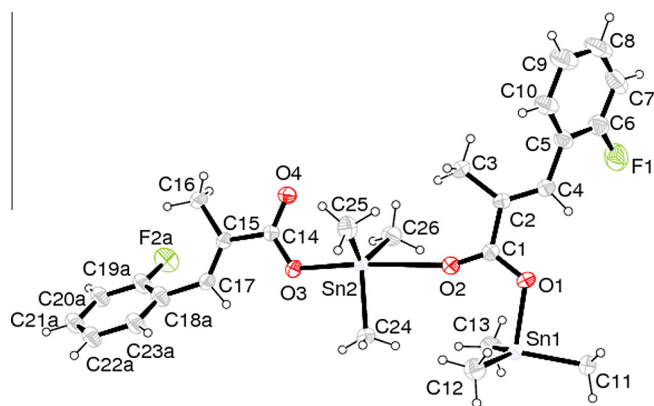


Fig. 3. Dimeric ORTEP diagram of complex 4.

Table 3
Selected bond lengths (Å) and bond angles (°) of complex 4.

Bond lengths (Å)			
Sn1–C11	2.107(6)	Sn1–O1	2.109(4)
Sn1–C12	2.107(5)	Sn2–O2	2.728(4)
Sn1–C13	2.103(6)	Sn2–O3	2.119(4)
O1–C1	1.292(6)	Sn2–C24	2.114(7)
O2–C1	1.225(6)	Sn2–C25	2.114(6)
		Sn2–C26	2.104(5)
Bond angles (°)			
O2–Sn2–O3	175.06(13)	C13–Sn–C12	126.6(2)
O1–Sn1–C11	91.34(19)	C13–Sn–C11	113.2(2)
O1–Sn1–C12	99.18(19)	C25–Sn2–C26	125.8(2)
O1–Sn1–C13	99.2(2)	C24–Sn2–C26	116.7(2)
C12–Sn–C11	116.0(2)	C24–Sn2–C25	113.4(2)

3.5.2. Antifungal studies

The ligand **HL** and its organotin(IV) complexes (**1–6**) were screened for antifungal activity against four fungal strains (*Aspergillus flavus*, *Aspergillus niger*, *Aspergillus fumigatus* and *Fusarium solani*) by using agar tube dilution method [18]. The results are shown in Fig. 6. *Terbinafine* was used as standard drug in this assay. Criteria for activity is based on percent growth inhibition; more than 70% was considered as significant activity, 60–70% as good, 50–60% as moderate while below 50% was considered as non-significant [37]. The antifungal data showed that compound **4** exhibited 100% growth inhibition against *Aspergillus niger*, *Aspergillus fumigatus* and *Fusarium solani* while significant against *Aspergillus flavus*. The compound **6** exhibited 100% growth inhibition against *Aspergillus niger* and *Aspergillus fumigatus* while significant against *Aspergillus flavus* and *Fusarium solani*. The compound **5** showed good to significant activity against *Aspergillus niger*, *Aspergillus fumigatus* and *Fusarium solani*. The compounds **1–3** showed non-significant to moderate activity against all the tested fungal strains. Like antibacterial activity, triorganotin(IV) compounds

aureus) and two Gram-negative (*Escherichia coli* and *Bordetella bronchiseptica*). The experiment was performed in triplicate by agar well-diffusion method [17]. *Roxythromycin* and *Cefixime* were used as positive control. The results are shown in Fig. 5. Criteria for activity is based on zone of inhibition (mm); inhibition zone more than 20 mm shows significant activity, for 18–20 mm inhibition activity is good, 15–17 mm is low, and below 11–14 mm is non-significant [37]. The antibacterial study demonstrates that compound **4** exhibited significant activity against Gram-negative bacteria (*Escherichia coli* and *Bordetella bronchiseptica*) and also greater than both reference drugs used while compounds **5** and **6** showed significant activity against all tested bacterial strains or even greater against some strains. The compounds **1–3** and ligand **HL** showed low to significant activity. In general, triorganotin(IV) compounds showed greater antibacterial activity than di-analogues which may be due to greater lipophilicity and permeability through the cell membrane which is consistent with literature [5,38,39].

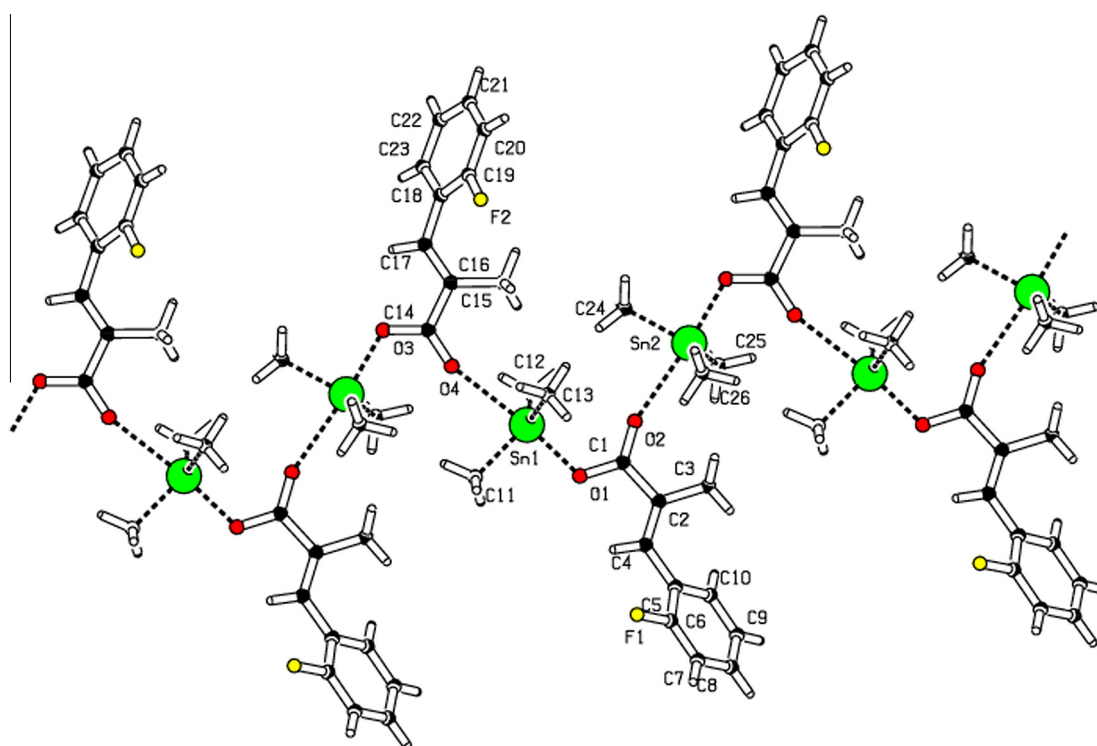


Fig. 4. Polymeric structure of complex 4.

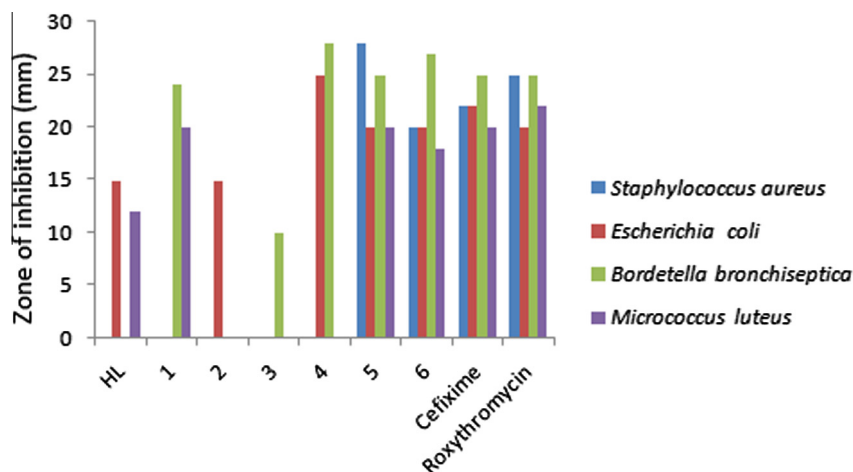


Fig. 5. Antibacterial activity of HL and its organotin(IV) complexes (1–6).

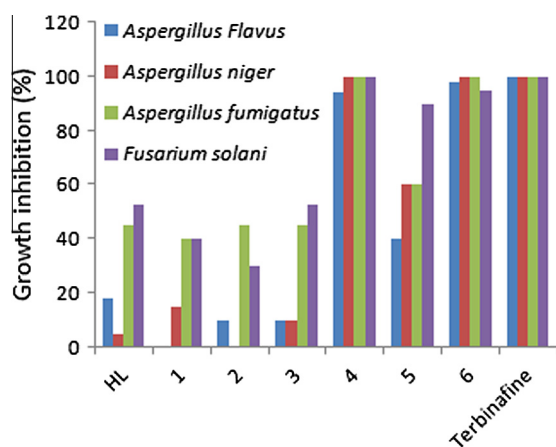


Fig. 6. Antifungal activity of HL and its organotin(IV) complexes (1–6).

showed greater antifungal activity than di-analogues which is also consistent with literature [5,40,41].

3.5.3. Cytotoxic studies

In vitro cytotoxicity of ligand **HL** and organotin(IV) complexes (1–6) was studied against the brine-shrimp lethality method [17] by using reference drug MS-222 (*Tricaine Methanesulfonate*) and the results are summarized in Fig. 7. The data is based on mean value of two replicates each of 10, 100 and 500 $\mu\text{g mL}^{-1}$. The LD_{50} data exhibited that compound 4–6 showed greater toxicity having LD_{50} values 0.008(4), 0.20(6) and 2.59(5) $\mu\text{g mL}^{-1}$ while compounds 1–3 exhibited less toxicity having LD_{50} values 313.1(1), 403(3) and 736(2) $\mu\text{g mL}^{-1}$.

3.6. Catalytic activity of organotin(IV) carboxylates

Organotin(IV) carboxylates were used as catalyst in a transesterification reaction of triglycerides in sesame oil with methanol to produce biodiesel (Fatty acid methyl esters – the chemical name of biodiesel). The organotin(IV) carboxylates were selected due to the Lewis acid character of tin atom. The tin atom has the property of coordination expansion which may play an important role in the catalytic activity of different substituted organotin compounds. Since Lewis acid can activate carbonyl groups which lead to increase in the electrophilicity of the carbonyl carbon in triglycerides and a subsequent interaction with tin atom.

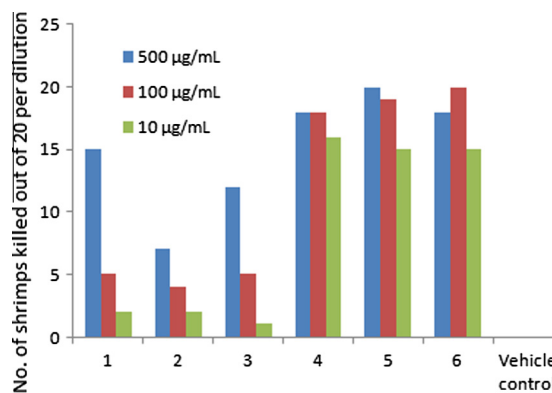


Fig. 7. Cytotoxicity of HL and its organotin(IV) complexes (1–6) against brine-shrimps (*in vitro*).

In the present study, the transesterification reaction of triglycerides in sesame oil was carried out in molar ratio of 400:100:1 (methanol:oil:catalyst) to assess the catalytic activity of organotin(IV) carboxylates [5]. The experimental conditions were not optimized and no attempt was made to remove the added catalyst from the reaction mixture. However, the effect of reaction time on % age conversion of triglycerides into fatty acid methyl esters (biodiesel) was studied but was not optimized to get the maximum % age conversion because the aim was to assess the catalytic activity of different organotin(IV) carboxylates. The sample was taken from the reaction mixture at regular interval of 1, 8, 16 and 24 h and was analyzed by ^1H NMR to calculate % age conversion of triglycerides into fatty acid methyl esters (biodiesel). The results are shown in Fig. 8. The equation used to quantify the extent of transesterification [42,43] was:

$$C = \frac{2A_{\text{Me}}}{3A_{\text{CH}_2}} \times 100$$

where C = percentage conversion of triglycerides to corresponding methyl esters, A_{Me} = integration value of the methoxy protons of the methyl esters, A_{CH_2} = integration value of α -methylene protons. The representative ^1H NMR spectrum showing % age conversion (80.9%) of oil (triglycerides) into biodiesel (fatty acid methyl esters) is shown in Fig. 9. The characteristic peak of methoxy protons was observed as a strong singlet at 3.65 ppm and a triplet of α - CH_2 protons at 2.26 ppm. These two peaks are the distinct peaks for the confirmation of conversion of oil (triglycerides) into biodiesel (fatty acid methyl esters) [13]. The results demonstrated that

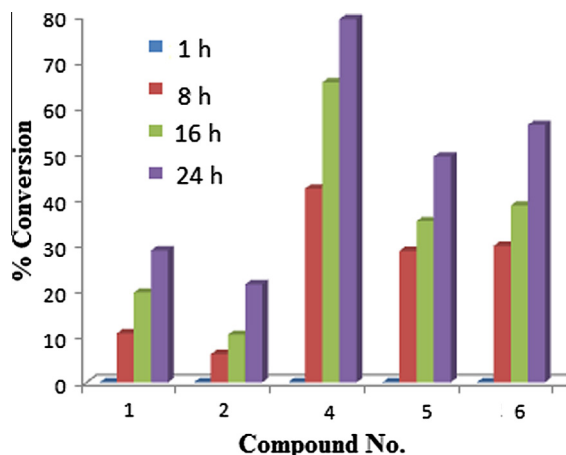


Fig. 8. % Age conversion of sesame oil triglycerides into FAMES (biodiesel).

catalytic activity was increased with increase in time interval and triorganotin(IV) carboxylates (compounds **4–6**) gave better % conversion than diorganotin(IV) carboxylates. Out of triorganotin(IV) carboxylates (compounds **4–6**), the compound **4** (trimethyltin(IV) derivative) gave highest conversion 80.9% in 24 h which may be

due to presence of small methyl groups causing less hindrance during attack on bulky triglyceride molecules.

3.7. DNA binding studies

The binding interaction of the SS-DNA with ligand **HL** and complexes **1** and **4** was investigated by comparing their absorption spectra with and without SS-DNA. Both the ligand **HL** and complexes **1** and **4** showed minor bathochromic shift of the spectral band with significant hypochromicity, suggesting mainly intercalating mode of binding as well as groove binding tendency of the compounds to the DNA helix (Figs. 10–12). This may be attributed to the presence of phenyl group that facilitates the interaction with double stranded DNA [43]. After 24 h, the spectrum was again taken and obtained the same results which confirm the stability of drug–DNA adduct.

The intrinsic binding constant K of the ligand **HL** and complexes **1** and **4** were calculated in order to compare binding strengths of ligand–DNA and complex–DNA by using Benesi–Hildebrand equation [20]:

$$\frac{A_0}{A - A_0} = \frac{\epsilon_G}{\epsilon_{H-G} - \epsilon_0} + \frac{\epsilon_G}{\epsilon_{H-G} - \epsilon_G} \times \frac{1}{K[\text{DNA}]}$$

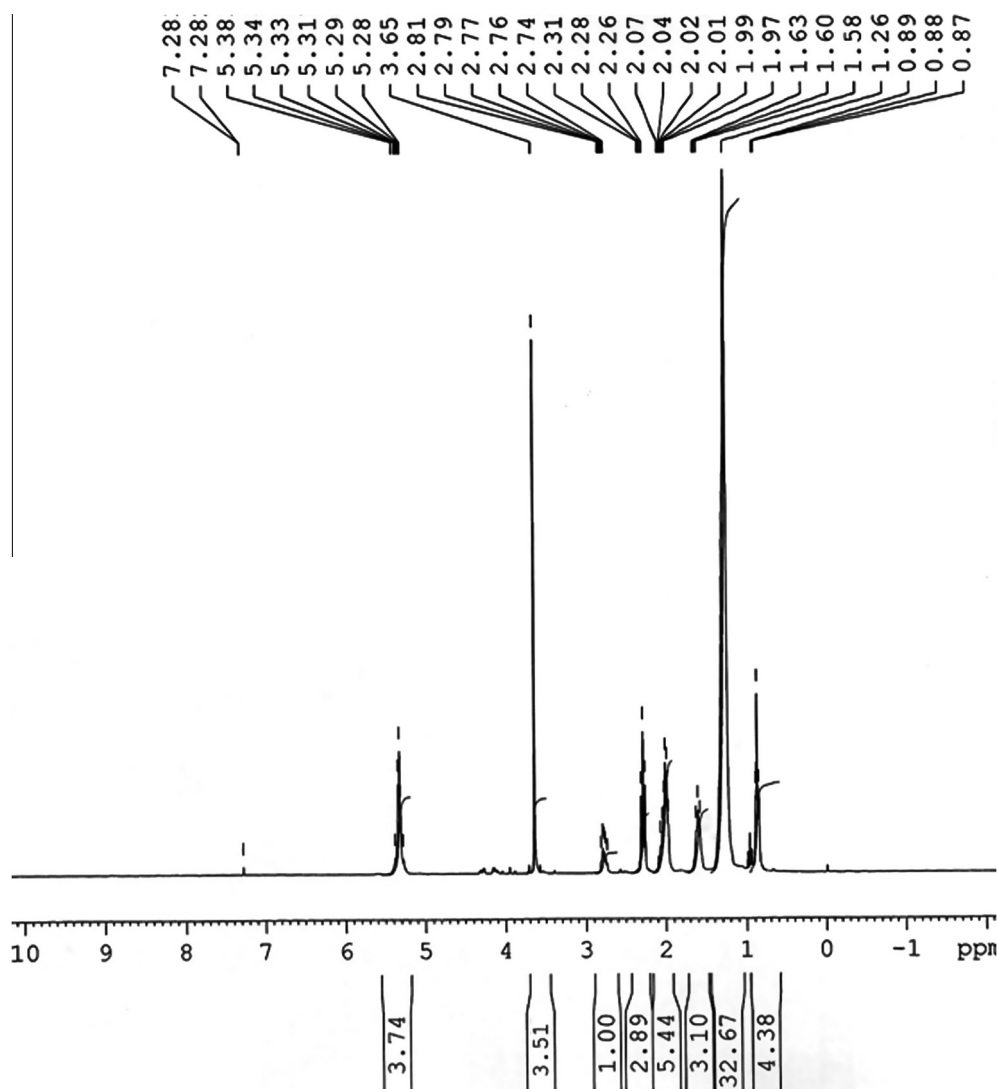


Fig. 9. ^1H NMR spectrum showing formation of biodiesel with 80.9% conversion of oil (triglycerides) into biodiesel (fatty acid methyl esters).

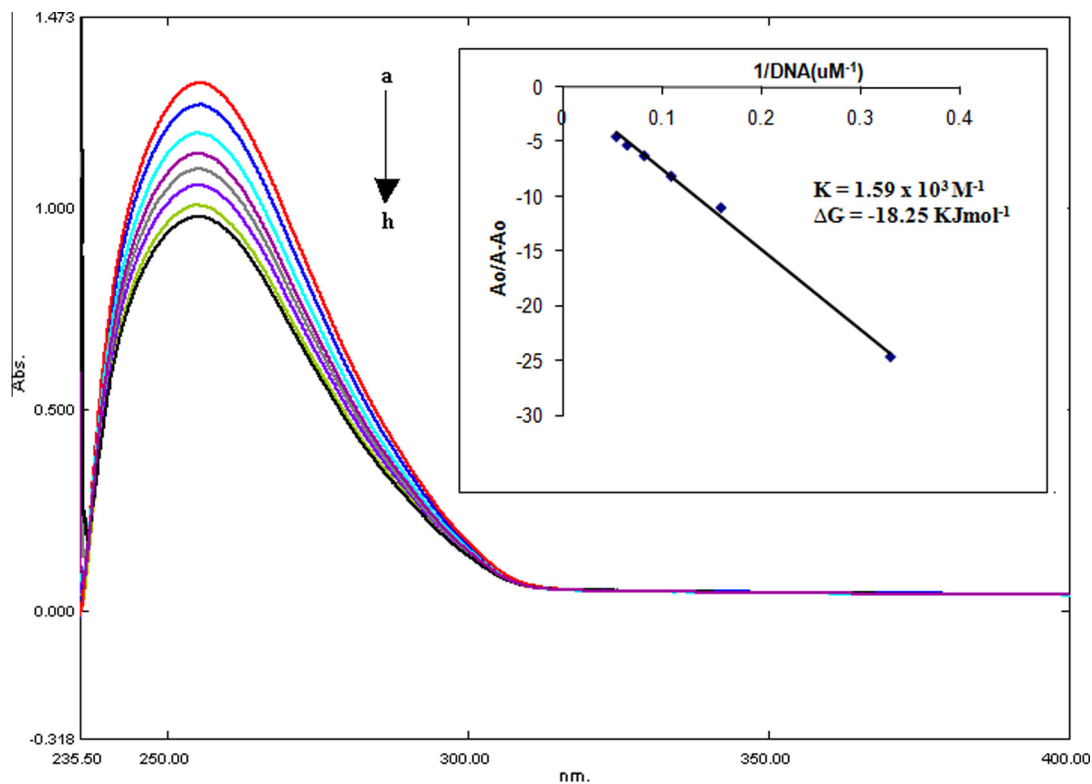


Fig. 10. Absorption spectra of 20 μM HL in the absence (a) and presence of 3 μM , (b) 6 μM , (c) 9 μM , (d) 12 μM , (e) 15 μM , (f) 18 μM , (g) and 21 μM , (h) DNA. The arrow direction indicates increasing concentrations of DNA. Inside graph is the plot of $A_0/(A-A_0)$ vs. $1/[DNA]$ for the determination of binding constant and Gibb's free energy of HL-DNA adduct.

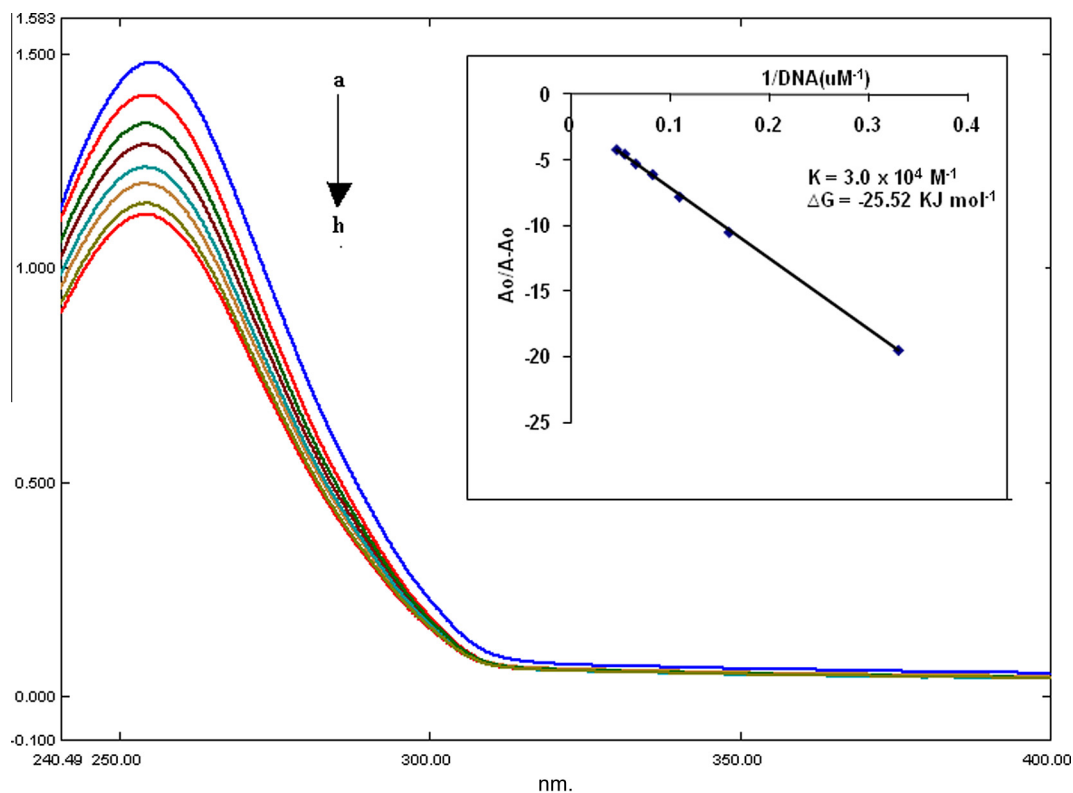


Fig. 11. Absorption spectra of 20 μM complex 1 in the absence (a) and presence of 3 μM , (b) 6 μM , (c) 9 μM , (d) 12 μM , (e) 15 μM , (f) 18 μM , (g) and 21 μM , (h) DNA. The arrow direction indicates increasing concentrations of DNA. Inside graph is the plot of $A_0/(A-A_0)$ vs. $1/[DNA]$ for the determination of binding constant and Gibb's free energy of complex 1-DNA adduct.

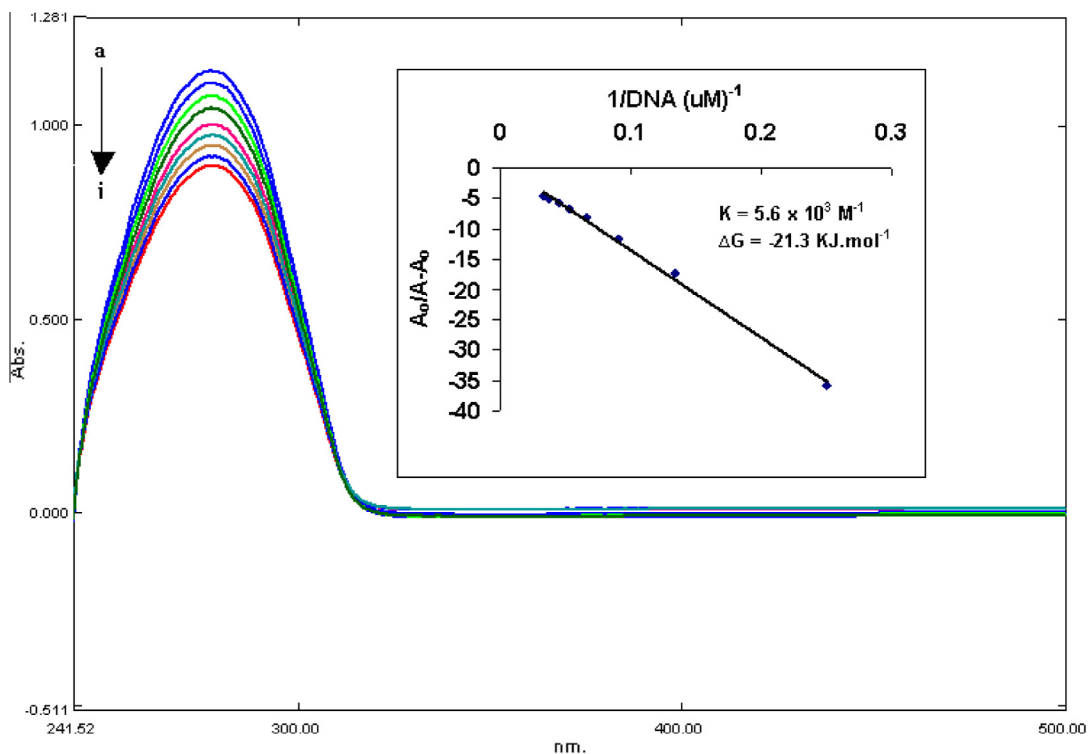


Fig. 12. Absorption spectra of 20 μM complex **4** in the absence (a) and presence of 3 μM , (b) 6 μM , (c) 9 μM , (d) 12 μM , (e) 15 μM , (f) 18 μM , (g) 21 μM , (h) and 24 μM , (i) DNA. The arrow direction indicates increasing concentrations of DNA. Inside graph is the plot of $A_0/(A-A_0)$ vs. $1/[\text{DNA}]$ for the determination of binding constant and Gibb's free energy of complex **4**–DNA adduct.

where K = binding constant, A_0 = absorbance of the drug, A = absorbance of the drug and its complex with DNA, ε_G = absorption coefficient of the drug, ε_{H-G} = absorption coefficient of the drug–DNA complex.

The binding constants were obtained from the intercept-to-slope ratios of $A_0/(A-A_0)$ versus $1/[\text{DNA}]$ plots. The binding constants were found to be $1.59 \times 10^3 \text{ M}^{-1}$ (**HL**), $3.0 \times 10^4 \text{ M}^{-1}$ (**1**) and $5.6 \times 10^3 \text{ M}^{-1}$ (**4**).

The Gibb's free energy (ΔG) of the ligand **HL** and complexes **1** and **4** were determined by using the following equation:

$$\Delta G = -RT \ln K$$

where R is general gas constant ($8.314 \text{ J K}^{-1} \text{ mol}^{-1}$) and T is the temperature (298 K). The Gibb's free energies were found -18.25 (**HL**), -25.52 (**1**), and $-21.3 \text{ kJ mol}^{-1}$ (**4**), indicating spontaneous interaction of the compounds with DNA.

4. Conclusions

A series of six organotin(IV) carboxylate complexes of 3-(2-fluorophenyl)-2-methylacrylic acid were synthesized and characterized by FT-IR, NMR (^1H and ^{13}C). The complexes **1** and **4** were also analyzed by single crystal X-ray analysis. The complex **1** has shown hexa co-ordinated behaviour with distorted octahedral geometry in both solution and solid state. The complex **4** has shown four co-ordinated behavior in solution state while five coordinated with distorted trigonal bipyramidal geometry in solid state. The antimicrobial results showed that triorganotin(IV) carboxylates **4–5** exhibited greater antibacterial and antifungal activity than diorganotin(IV) carboxylates **1–3**. The greater antimicrobial activity of triorganotin(IV) derivatives may be due to greater lipophilic character which cause easy passage of organotin moieties into the microbial cells leading to death of pathogen cells. The cytotoxic studies revealed that complexes **4–6** were

shown more toxicity having LD_{50} values in the range 0.008 – $2.59 \mu\text{g mL}^{-1}$. The significant hypochromicity was observed in DNA binding studies of ligand **HL** and complexes **1** and **4** which may be due to minor groove as well as intercalating mode of binding with base pairs of DNA. The triorganotin(IV) carboxylates **4–6** were shown better catalytic activity than their di- analogues **1–2**. Out of triorganotin(IV) carboxylates **4–6**, the complex **4** (trimethyltin(IV) derivative) showed greater catalytic activity which may be due to presence of small methyl groups causing less hindrance during attack on bulky triglyceride molecules.

Acknowledgment

M. Tariq (Pin No. 074-0616-Ps4-099) is thankful to higher education commission of Pakistan for financial support during the present study.

Appendix A. Supplementary data

CCDC 910965 and 910967 contains the supplementary crystallographic data for **1** and **4**. These data can be obtained free of charge via <http://www.ccdc.cam.ac.uk/conts/retrieving.html>, or from the Cambridge Crystallographic Data Centre, 12 Union Road, Cambridge CB2 1EZ, UK; fax: +44 1223 336 033; or e-mail: deposit@ccdc.cam.ac.uk.

References

- [1] V. Chandrasekhar, S. Nagendran, V. Baskar, *Coord. Chem. Rev.* 235 (2002) 1.
- [2] N. Muhammad, A. Shah, Z. Rehman, S. Shuja, S. Ali, R. Qureshi, A. Meetsma, M.N. Tahir, *J. Organomet. Chem.* 694 (2009) 3431.
- [3] L. Pellerito, L. Nagy, *Coord. Chem. Rev.* 224 (2002) 111.
- [4] F.W. Van Der Weij, *Macromol. Chem. Phys.* 181 (1980) 2541.
- [5] S. Karpel, *Tin Uses* 149 (1986) 1.

- [6] P. Fierens, G.V.D. Dunghen, W. Segers, R.V. Elsuwe, *React. Kinet. Lett.* 85 (1978) 179.
- [7] M. Gielen, *Coord. Chem. Rev.* 151 (1996) 41.
- [8] M. Hanif, M. Hussain, S. Ali, M.H. Bhatti, M.S. Ahmed, B. Mirza, H.S. Evans, *Turk. J. Chem.* 31 (2007) 349.
- [9] C. Vatsa, V.K. Jain, T. Kesavadas, E.R.T. Tiekink, *J. Organomet. Chem.* 410 (1991) 135.
- [10] E.R.T. Tiekink, *J. Appl. Organomet. Chem.* 5 (1991) 1.
- [11] S. Shahzadi, S. Ali, *J. Iran. Chem. Soc.* 5 (2008) 16.
- [12] J. Otera, *J. Org. Chem.* 56 (1991) 5307.
- [13] M. Tariq, S. Ali, F. Ahmad, M. Ahmad, M. Zafar, N. Khalid, M.A. Khan, *Fuel Process. Technol.* 92 (2011) 336.
- [14] M. Ahmad, K. Ullah, M.A. Khan, M. Zafar, M. Tariq, S. Ali, S. Sultana, *Energy Sources Part A* 14 (2011) 1365.
- [15] M. Ahmad, S. Samuel, M. Zafar, M.A. Khan, M. Tariq, S. Ali, S. Sultana, *Energy Sources Part A* 14 (2011) 1386.
- [16] D.D. Perrin, W.L.F. Armengo, *Purification of Laboratory Chemicals*, third ed., Pergamon Press, Berlin, Oxford, 2003.
- [17] A. Rehman, M.I. Choudhary, W.J. Thomsen, *Bioassay Techniques for Drug Development*, Harwood Academic Publishers, Amsterdam, The Netherlands, 2001.
- [18] B.N. Mayer, N.R. Ferrigni, J.E. Putnam, L.B. Jacobson, D.E. Nichols, J.L. McLaughlin, *Plant. Med.* 45 (1982) 31.
- [19] Y. Zhang, X. Wang, L. Ding, *Nucleosides, Nucleotides Nucleic Acids* 30 (2011) 49.
- [20] C.V. Sastri, D. Eswaremoorthy, L. Giribabu, B.G. Maiya, *J. Inorg. Biochem.* 94 (2003) 138.
- [21] S.G. Teoh, S.H. Ang, J.P.D. Declercq, *Polyhedron* 16 (1997) 3729.
- [22] X.N. Fang, X.Q. Song, Q.L. Xie, *J. Organomet. Chem.* 619 (2001) 43.
- [23] H.D. Yin, C.H. Wang, Q.J. Xing, *Polyhedron* 23 (2004) 1805.
- [24] H.D. Yin, C.H. Wang, Y. Wang, C.L. Ma, J.X. Shao, J.H. Zhang, *Acta Chim. Sin.* 60 (2002) 143.
- [25] M.H. Bhatti, S. Ali, H. Masood, M. Mazhar, S.I. Qureshi, *Synth. React. Inorg. Met.-Org. Chem.* 30 (2000) 1715.
- [26] S. Ali, F. Ahmad, M. Mazhar, A. Munir, M.T. Masood, *Synth. React. Inorg. Met.-Org. Chem.* 32 (2001) 357.
- [27] F. Ahmad, S. Ali, M. Parvez, A. Munir, M. Mazhar, K.M. Khan, T.A. Shah, *Heteroat. Chem.* 13 (2002) 638.
- [28] M. Danish, S. Ali, A. Badshah, M. Mazhar, H. Masood, A. Malik, G. Kehr, *Synth. React. Inorg. Met.-Org. Chem.* 27 (1997) 863.
- [29] E.R.T. Tiekink, *Trends Organomet. Chem.* 1 (1994) 71.
- [30] S.W. Ng, C. Wei, V.G.K. Das, T.C.W. Mak, *J. Organomet. Chem.* 334 (1987) 295.
- [31] M. Hussain, Z. Rehman, M. Hanif, M. Altaf, A. Rehman, S. Ali, K.J. Cavell, *J. Appl. Organomet. Chem.* 25 (2011) 412.
- [32] M. Parvez, S. Ali, T. Masood, M. Mazhar, M. Danish, *Acta Crystallogr., Sect. C* 53 (1997) 1211.
- [33] A. Ruzicka, L. Dostal, R. Jambor, V. Buchta, J. Brus, *J. Appl. Organomet. Chem.* 16 (2002) 315.
- [34] C.L. Ma, Q.F. Zhang, R.F. Zhang, L.L. Qiu, *J. Organomet. Chem.* 690 (2005) 3033.
- [35] N. Muhammad, Z. Rehman, S. Shujah, A. Shah, S. Ali, A. Meetsma, Z. Hussain, *J. Coord. Chem.* 65 (2012) 3766.
- [36] A.W. Addison, R.T. Nageswara, J. Reedijk, R.J. Van, G.C. Verschoor, *J. Chem. Soc., Dalton Trans.* 7 (1984) 1349.
- [37] M. Sirajuddin, S. Ali, A. Haider, N.A. Shah, A. Shah, M.R. Khan, *Polyhedron* 40 (2012) 19.
- [38] S. Shahzadi, K. Shahid, S. Ali, M. Bakhtiar, *Turk. J. Chem.* 32 (2008) 333.
- [39] S. Ahmed, M.H. Bhatti, S. Ali, F. Ahmed, *Turk. J. Chem.* 30 (2006) 471.
- [40] S. Hadi, B. Irawan, *J. Appl. Sci. Res.* 4 (2008) 1521.
- [41] J.J. Bonire, G.A. Ayoko, P.F. Olurinola, J.O. Ehinmidu, N.S.N. Jalil, A.A. Omachi, *Met.-Based Drugs* 5 (1998) 233.
- [42] G. Gelbard, O. Bres, R.M. Vargas, F. Vielfaure, U.F. Schuchardt, *J. Am. Oil Chem. Soc.* 72 (1995) 1239.
- [43] K.S. Prasad, L.S. Kumar, K.B. Vinay, S.C. Shekar, B. Jayalakshmi, H.D. Revanasiddappa, *Int. J. Chem. Res.* 2 (2011) 1.